Available online at www.sciencedirect.com

ScienceDirect

www.elsevier.com/locate/jes

JES JOURNAL OF ENVIRONMENTAL SCIENCES

www.jesc.ac.cn

Screening ionic liquids for efficiently extracting perfluoroalkyl chemicals (PFACs) from wastewater

Kaihang Zhang[1,*], *David Kujawski*[2], *Chris Spurrell*[3], *Bing Wang*[4,*], *John C. Crittenden*[1]

[1] *Brook Byers Institute of Sustainable Systems and School of Civil and Environmental Engineering, Georgia Institute of Technology, Atlanta, GA 30332, USA*

[2] *Refinery Water Engineering and Associates, Hydrocarbon Processing Water and Waste Technology, Inc., Houston, TX 77042, USA*

[3] *Chevron USA, Vancouver, WA 98664, USA*

[4] *School of Municipal and Environmental Engineering, Shenyang Jianzhu University, Shenyang 110000, China*

ARTICLE INFO

Article history:
Received 1 August 2022
Revised 18 August 2022
Accepted 19 August 2022
Available online 30 August 2022

Keywords:
Conductor-like screening model for real solvents (COSMO-RS)
Ionic liquids
Perfluorooctanoic acid (PFOA)
Perfluorooctane sulfonic acid (PFOS)
Liquid-liquid extraction

ABSTRACT

Liquid-liquid extraction (LLE) using ionic liquids (ILs)-based methods to remove perfluoroalkyl chemicals (PFACs), such as perfluorooctanoic acid (PFOA) and perfluorooctane sulfonic acid (PFOS), from wastewater, is an important strategy. However, the lack of physicochemical and LLE data limits the selection of the most suitable ILs for the extraction of PFACs. In this work, 1763 ILs for PFACs extraction from water were systematically screened using COSMOtherm to estimate the infinite dilution activity coefficient ($\ln\gamma^{\infty}$)of PFOA and PFOS in water and ILs. To evaluate the accuracy of COSMOtherm, 8 ILs with various $\ln\gamma^{\infty}$ values were selected, and their extraction efficiency (E) and distribution coefficient (D_{exp}) were measured experimentally. The results showed that the predicted $\ln\gamma^{\infty}$ decreased as the increase of experimental extraction efficiency of PFOA or PFOS, while the tendency of predicted distribution coefficient (D_{pre}) was consistent with the experimental (D_{exp}) results. This work provides an efficient basis for selecting ILs for the extraction of PFACs from wastewater.

Introduction

Perfluoroalkyl chemicals are a group of chemically stable compounds that owe their stability to strong C-F bonds. As a result, they are persistent in the environment, which leads to bioaccumulation and adverse effects on ecosystems and human health (Qian et al., 2016). Among them, perfluorooctanoic acid (PFOA) and perfluorooctane sulfonic acid (PFOS) have been recognized as the persistent organic pollutant (POP) at the fourth meeting of the Stockholm Convention (Wang et al., 2009). After 2002, the production of PFOA and PFOS declined, and they were gradually banned in Western countries. However, they are still being produced in many developing coun-

* Corresponding authors.
E-mails: kzh@gatech.edu (K. Zhang), 18202460111@163.com (B. Wang).

https://doi.org/10.1016/j.jes.2022.08.025
1001-0742/

tries (Zhou et al., 2013) and are widely used in clothing treatments, leather products, and the semiconductor industry (Arias et al., 2015). In practical, we could not eliminate fluorinated chemicals, therefore the efficient removal of perfluoroalkyl chemicals (PFACs) from wastewater will be required and is challenging in the foreseeable future.

The conventional treatment methods are inefficient or economically infeasible (Bao et al., 2014). For example, coagulation treatment with alum or other multivalent metals is ineffective at removing PFACs (Chen et al., 2017). Granular activated carbon (GAC) has a large adsorption capacity, but its performance declines quickly and requires frequent replacement or reactivation, leading to high treatment costs (Chiavola et al., 2020). Ion exchange method can be used to absorb PFACs, and the lifetime of ion exchange column is ten times longer than GAC, but it has the disadvantage of being much more expensive than GAC (Senevirathna et al., 2010). Another main direction is defluorination. The most widely used methods are activated sludge or advanced oxidation processes (AOPs), which remain inefficient due to their limited oxidation or reduction capacity (Bentel et al., 2020). To overcome the problem, recently, UV/persulfate and vacuum ultra-violet (VUV) radiation have been applied for PFAC treatment. The most challenging aspects of those methods are the formation of secondary harmful byproducts and the low energy efficiency of VUV radiation (Bao et al., 2018). The electrochemical advanced oxidation process (EAOP) is an emerging technology that can oxidize organics with direct and indirect oxidation. It can break down PFOA or PFOS into short-chain PFACs, but still cannot achieve complete mineralization (Lin et al., 2018; Niu et al., 2016). In view of the problems existing in the above methods, as well as the extremely low concentration of PFACs in the real wastewater (mg/L or μg/L level), it is quickly realized that the enrichment of PFACs by pretreatment using extraction methods is a reasonable strategy.

The extraction of PFACs using common organic solvents such as octanol or long-chain polymers has been demonstrated to be ineffective (Zhang et al., 2021). Ionic liquids (ILs) are promising solvents composed of organic cations and organic or inorganic anions (Li et al., 2021; Zhang, 2020). The countless combinations of those cations and anions allow engineering the ILs properties for specific purposes (Sun et al., 2020). In our case, the solubility of ILs can be regulated by selecting cations and anions with different hydrophobicity, which has been successfully utilized for the liquid-liquid extraction (LLE) of rare-earth metals, organic acids, esters, aromatic hydrocarbons, etc. (Chen et al., 2021; Skoronski et al., 2020; Li et al., 2019; Yokozeki and Shiflett, 2010). Compared to other extraction methods, LLE offers the greatest energy savings and is very easy to operate, while LLE is a non-destructive method of removing PFOA/PFOS and can easily be reused after reverse extraction. The octanol-water partition coefficient (K_{ow}) is a critical metric to evaluate its feasibility. The log K_{ow} for PFOS is about -0.18, indicating that its extraction from the aqueous phase into an organic phase is quite difficult (Costanza et al., 2019). However, some ILs (e.g., Fe_3O_4-cyclodextrin IL) have strong electrostatic and hydrophobic interactions with PFOA and PFOS (Badruddoza et al., 2017). Accordingly, LLE with IL as an extractant to extract PFOA from the aqueous was reported in our previous work (Zhang et al., 2021), finding that specific ILs substantially improved the extraction efficiency in octanol water extraction setup. The selected ILs should be insoluble in aqueous to prevent secondary pollution to the water phase and, simultaneously, to extract the PFACs into the organics.

These two requirements could translate to two important criteria: (1) high activity coefficients of ILs in water, and (2) low activity coefficient for PFOA or PFOS in ILs (Zhang et al., 2021). To be noticed, as both PFOA and PFOS are surfactants, the extractant must be hydrophobic (i.e., have a large activity coefficient) to prevent extreme emulsification. Therefore, a low $\ln\gamma^{\infty}$ of PFACs in IL (lower γ^{∞} corresponding to higher solubility) is needed. Numerous possible ILs can be synthesized by the combination of cations and anions. It would be costly to synthesize and characterize all of them. Thus, an initial screening method for selecting ILs is essential.

The conductor-like screening model for real solvents (COSMO-RS) is suitable for fast thermodynamic calculations and screening parameters, such as γ^{∞} (Austin et al., 2018; Coto et al., 2021; Zhao et al., 2022; Dai et al., 2021; Olea et al., 2021; Louwen et al., 2020; Arenas et al., 2022; Pye et al., 2009; Song et al., 2017; Xiong et al., 2014; Wu et al., 2021). The COSMO-RS predicted γ^{∞} had been compared with other common solvent selection methods like the Hildebrand parameter and the Hansen solubility parameters. The results indicate that COSMO-RS is a more reliable tool for fast solvent selection (Brouwer and Schuur, 2019; Liu et al., 2021). The COSMO-RS model relies on the sigma profile (σ-profile) data, calculated from the molecular structure and electronic densities determined by the quantum chemical calculations based on density function theory (DFT) (Klamt et al., 2010; Mullins et al., 2006). Several studies have reported that the COSMO-RS model can be used to calculate the physicochemical properties of PFACs. For example, the COSMO-RS calculated membrane-water partition coefficient (K_{mw}) results aligned with the experimental K_{mw} values for C8-C14 alkyl chains, although it underestimated the impacts of the CF_2 and CH_2 increments and C4-C8 PFAS anions (Droge et al., 2019). pK_a estimates from COSMO-RS for carboxylic acids and fluorinated carboxylic acids (including PFOA and its related short-chain substances) show differences between calculated and experimental pK_a in the range of $\pm$ 0.5 log unit (Goss, 2008; Wang et al., 2011). Therefore, COSMO-RS is a promising method for determining the physicochemical properties of PFOA and PFOS. To the best of our knowledge, the COSMO-RS method has so far focused on the impact of chain length on the physical and chemical properties of fluorinated compounds, and no studies regarding the extraction of PFOA and PFOS using ILs have been reported.

The objective of this work is to develop a method for screening the potential ILs for extracting PFOA and PFOS from wastewater. COSMO-RS was used to determine the $\ln\gamma^{\infty}$ for 1763 ILs, consisting of 41 kinds of cations with 8 types of imidazolium, pyridinium, morpholinium, pyrrolidinium, choline, amine, ammonium, phosphonium, and 43 kinds of anions with different H-bond alkaline, hydrophilic/hydrophobic properties, and etc. The primary goal of this analysis was to screen appropriate ILs for LLEs of PFOA and PFOS using COSMO-RS. To verify the screening method, the properties of a small number of ILs with various γ^{∞} values predicted by COSMOtherm were compared with the experimental results.

1. Materials and methods

1.1. Computational details

COSMO-RS calculations were performed using COSMOtherm software (version 19.0.4, release 5528, using the parameters BP_TZVP_19, COSMOlogic (Leverkusen, Germany)), with the reported standard methods (Liu et al., 2020). The temperature was set at 298 K in our modeling. The first step in the COSMO-RS prediction procedure is to apply the continuum solvation model COSMO to simulate a virtual conductor environment for the molecule of interest. The screening charge density (σ) is then obtained by standard quantum chemical calculations. σ is the charge density observed outside the continuous dielectric solvent surface with the unit of e/Å^2, which is the average electron charge number. The three-dimensional (3D) distribution of the screening charge density on the surface of each molecule is converted into a surface composition function, called the σ-profile. For the second step, the statistical thermodynamics of molecular interactions is performed in the COSMOtherm software. σ and σ′ are the screening charges of two interacting surface segments. $P(\sigma)$ is the probability distribution of a specific charge density on a molecular surface segment. The interaction energy of surface pairs (E_{vdW}, $E_{H\text{-}Bond(HB)}$, and $E_{misfit\ (MF)}$, misfit represents electrostatic force) are specified in terms of their respective screening charge densities σ and σ′. The chemical potential μ of σ, referred to as the σ-potential, was computed using Eq. (1) as below:

$$\mu(\sigma) = -\frac{RT}{a_{eff}}\ln\left(\int P(\sigma')\exp\left(\frac{a_{eff}}{RT}\mu(\sigma') - \frac{E_{vdW}(\sigma,\sigma')}{RT} - \frac{E_{HB}(\sigma,\sigma')}{RT} - \frac{E_{MF}(\sigma,\sigma')}{RT}\right)d\sigma'\right) \quad (1)$$

where, a_{eff} stands for the effective contact area, and $P(\sigma')$ represents the surface screening charge distribution of the whole system. Chemical potential (μ(σ)) of a compound is calculated from the integration of the σ-potential over the surface of the molecule.

Eq. (2) shows the μ of PFACs in water or ILs. At equilibrium, the μ values in the two phases should be equal, therefore the predicted distribution coefficient of $D_{i,pre}$ is proportional to the ratio of $\gamma_{i,L}$ to $\gamma_{i,w}$ (Eq. (3)) (Schwarzenbach et al., 2016). In this study, the concentration of PFACs was at ppm levels. Hence, $\gamma_{i,L}$ and $\gamma_{i,w}$ were approximately equal to γ^{∞} as calculated by COSMO-RS. For simplicity, the ratio of $\gamma^{\infty}_{i,w}$ to $\gamma^{\infty}_{i,L}$ is defined as $D^{*}_{i,pre}$. Further, the relative selectivity $S^{*}_{i,j,pre}$ can be calculated by Eq. (4).

$$\mu_i = \mu_i^0 + RT\ln\gamma_i x_i \quad (2)$$

$$D_{i,pre} = \frac{x_{i,L}}{x_{i,w}} = A_i\frac{\gamma_{i,w}}{\gamma_{i,L}} \approx A_i\frac{\gamma^{\infty}_{i,w}}{\gamma^{\infty}_{i,L}} \propto \frac{\gamma^{\infty}_{i,w}}{\gamma^{\infty}_{i,L}} = D^{*}_{i,pre} \quad (3)$$

$$S_{i,j,pre} = \frac{D_{i,pre}}{D_{j,pre}} \propto \frac{D^{*}_{i,pre}}{D^{*}_{j,pre}} = S^{*}_{i,j,pre} \quad (4)$$

where μ is the chemical potential, 0 expresses the standard state; γ is the activity coefficient; x is mole fraction; D and S represent the distribution coefficient and selectivity, respectively, D^* and S^* are the proportional relative value of the actual distribution coefficient and selectivity; i and j denote the different compounds, w and L stand for the aqueous phase and the IL phase, respectively; A is a constant value, which equals to $\exp((\mu^0_{i,L} - \mu^0_{i,w})/RT)$.

From the viewpoint of thermodynamics, there is a certain degree of ionization for PFACs in water, however, the ionization equilibrium constant is a fixed value at a certain temperature, while in the ILs phase, they mainly exist as the molecular form. In our previous work (Zhang et al., 2021), it has also been put forward that most of the PFOA in the aqueous solution could be extracted into the organic solution in the form of molecule. Therefore, the extraction process of PFACs is the distribution equilibrium of PFACs molecules in the two phases. According to Eq. (4), the selectivity $S_{i,j,pre}$ should be a value of $S^{*}_{i,j,pre}$ multiplied by a constant, relating to the A_i/A_j and the ionization equilibrium constants of i and j in the aqueous phase. For simplicity, in this work, $S^{*}_{i,j,pre}$ is applied to screen the ILs extractants, which will not affect the sequence of the predicted extraction efficiency. Thus, from the point of qualitative screening and prediction, the strategy provided in this study is practically effective.

In COSMO-RS calculation, PFOA and PFOS are treated as molecular compounds. COSMOfiles are required for all the PFOA, PFOS, water, ILs cations, and anions for the COSMO-RS prediction. All studied ILs were treated in an electroneutral way, i.e., each IL was treated as two different compounds in a stoichiometric mixture. The names and structures of PFOA and PFOS are provided in Appendix A Table S1, while cations and anions of ILs are listed in Appendix A Tables S2 and S3, respectively. Among them, the components marked in gray in Appendix A Tables S1-S3 were calculated according to the method described in the literature (Liu et al., 2020). The COSMOfiles for other components in this work were taken from the COSMO-RS database.

1.2. Experimental details

1.2.1. Materials

PFOA and PFOS were supplied by Shanghai Aladdin Biochemical Technology Co., Ltd. $[N_{8881}][Tf_2N]$ (98.0 wt.% purity) and $[N_{8881}][BF_4]$ (98.0 wt.% purity) were bought from Lanzhou Institute of Chemical Physics. $[N_{8881}][PF_6]$ (99.0 wt.% purity), $[N_{1114}][Tf_2N]$ (99.0 wt.% purity), $[N_{1114}][BF_4]$ (99.0 wt.% purity), $[N_{1114}][PF_6]$ (99.0 wt.% purity), [BMIM][PF_6] (99.0 wt.% purity), and [BMIM][BF_4] (99.0 wt.% purity) were purchased from the Shanghai Aladdin Biochemical Technology Co., Ltd. The names and structures of ILs used in this work are shown in Appendix A Tables S2 and S3. The *n*-octanol used as the diluent for the ILs (99.99 wt.%, Sinopharm Chemical Reagent Co., Ltd., high purity) was used without further purification. High-purity Milli-Q water (resistivity > 18.2 MΩ cm and conductivity < 0.1 μS/cm) was used to prepare all aqueous solutions. The information of the used chemicals is listed in detail in Appendix A Table S4.

1.2.2. Solution preparation

The extractive systems were prepared by diluting the ILs in *n*-octanol at a concentration of 1.25 mmol/L. The ILs + *n*-octanol, instead of pure ILs, were used as the extractive systems to avoid the formation of emulsification (Zhang et al., 2021).

The aqueous solutions were prepared by dissolving PFOA or PFOS in high-purity Milli-Q water, and the concentration of PFOA or PFOS was kept at 50 mg/L. All qualities were weighed using a METTLER analytical balance with an accuracy of ± 0.0001 g.

1.2.3. *Extraction procedure*

Extraction experiments were carried out in 20 mL flasks. The optimized extraction conditions reported in our previous work (Zhang et al., 2021) were adopted presently with IL of 1.25 mmol/L, PFOA/PFOS of 50 mg/L, volume ratio of the organic solution to the aqueous solution 1:1, the temperature at 298 K, and extraction time of 30 min. The volume of the aqueous phase was equal to that of the *n*-octanol phase. The detailed steps were as follows:

(1) The flasks were immersed in a temperature-controlled water bath. The initial pH for the aqueous solution was measured, then the organic phase was mixed with the aqueous solution and stirred for 30 min to reach equilibrium.
(2) The mixture was centrifuged at 4000 r/min for 5 min. After separating the mixture, the equilibrium pH for the aqueous solution and the volume of the two phases were measured.
(3) PFOA or PFOS remaining in the aqueous phase was measured by high-performance liquid chromatography (HPLC) and mass spectroscopy (MS). According to the data obtained, the extraction efficiency of PFOA (E_{PFOA}) or PFOS (E_{PFOS}) and the experimental distribution coefficient of PFOA or PFOS (D_{exp}) were determined by Eqs. (5) and (6), respectively.

$$E_i = \frac{C_{0,i} \times V_{0,w} - C_{e,i} \times V_{e,w}}{C_{0,i} \times V_{0,w}} \quad (5)$$

$$D_{i,exp} = \frac{C_{e,i\ in\ IL}}{C_{e,i\ in\ water}} \approx \frac{E_i}{1 - E_i} \quad (6)$$

where C is the concentration of PFOA or PFOS (mg/L), the subscripts 0 and e denote the initial and equilibrated concentrations of PFOA or PFOS in the aqueous solution; i represents PFOA or PFOS; V (L) is the volume of aqueous phase, and the subscript w denotes the aqueous solution. Because the volume of IL phase and water phase before and after extraction is almost constant (less than 5%), so Eq. (4) is applied.

1.2.4. *Apparatus and measurements*

The concentration of PFOA in the aqueous phase was determined by HPLC-MS using an Agilent 1100 HPLC equipped with a Zorbax SB C18 column (Agilent Technologies, Santa Clara, USA). Electrospray ionization mass spectra (ESI-MS) of PFOS were obtained using a Waters/Micromass ZQ mass spectrometer (Manchester, UK) equipped with a Harvard Apparatus syringe pump. Mass spectra were obtained in negative ion detection mode with a unit mass resolution at a step of 1 (mass charge ratio, *m*/z) unit. The mass range for ESI experiments ranged from *m*/z = 100 to 1000.

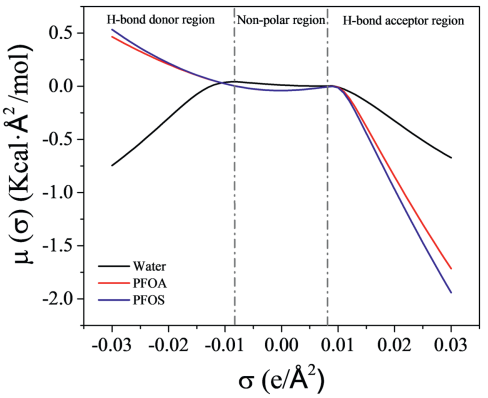

Fig. 1 – σ-potentials of water, perfluorooctanoic acid (PFOA), and perfluorooctanesulfonic acid (PFOS) predicted by conductor-like screening model for real solvents (COSMO-RS). The dashed vertical lines denote the 3 regions used to evaluate the H-bond donor region ($\sigma < -0.0082$ e/Å^2), non-polar region (-0.0082 e/Å$^2 < \sigma < 0.0082$ e/Å^2) and H-bond acceptor region ($\sigma > 0.0082$ e/Å^2). σ: the screening charge density. μ(σ): the chemical potential.

2. Results and discussion

2.1. *Evaluation of IL extraction efficiency using the COSMO-RS*

σ-potential is the polarization charge density, a thermodynamic property that qualitatively interprets the mixture's and their affinity towards another component (Eckert and Klamt, 2002; Jiang et al., 2021; Kurnia et al., 2015). In general, the σ-potential can be divided into three central regions: (1) H-bond donor region (where $\sigma < -0.0082$ e/Å^2, related to its ability to interact with H-bond donors), (2) non-polar region (where -0.0082 e/Å$^2 < \sigma < 0.0082$ e/Å^2), related to its ability to interact with non-polar groups (i.e., Van der Walls forces (VdW)), and (3) H-bond acceptor region (where $\sigma > 0.0082$ e/Å^2, related to its ability to interact with H-bond acceptors) (Rezaei Motlagh et al., 2020).

From Fig. 1, σ-potential values of PFOA and PFOS are more negative than that of water in the H-bond acceptor region, which means that PFOA and PFOS are strong H-bond acceptors. The non-polar region of PFOA and PFOS is lower than that of water due to their non-polar CF_3CF_n chains. It also confirms that the non-polar interactions through VdW forces are also essential for the extraction process, and the finding is consistent with our previous results using molecular dynamics (MD) simulations (Zhang et al., 2021). In brief, it is expected that the selected ILs can interact with PFOA or PFOS *via* the VdW forces and their strong H-bond acceptor groups.

For practical purposes in the selection of ILs, all three compounds in the system should be taken into account, i.e., PFOA, PFOS, and water. Therefore, we further predicted the $\ln\gamma^{\infty}$ of water, PFOA, and PFOS in ILs using COSMO-RS, and the results are shown in Figs. 2a-c. The color change from purple to red corresponds to an increase of $\ln\gamma^{\infty}$, corresponding to a de-

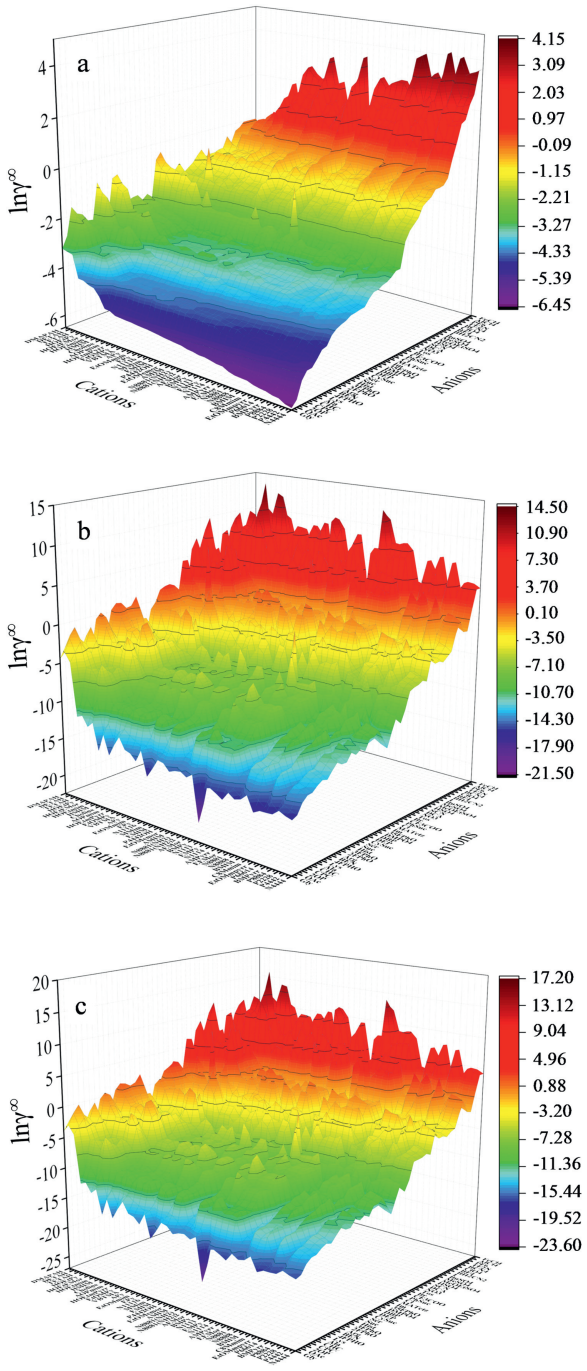

Fig. 2 – COSMO-RS prediction of the logarithmic infinite dilution activity coefficient ($\ln\gamma^{\infty}$) of (a) water, (b) PFOA, and (c) PFOS in ionic liquids (ILs) at 298 K. The full name of the cations and anions in Fig. 2 are provided in Appendix A Tables S2 and S3. The ILs used for the prediction can be combined freely by cations and anions.

crease in the solubility of water, PFOA, and PFOS in ILs. ILs with cations such as $[N_{1111}]^+$, $[EMPyrr]^+$, $[P_{2228}]^+$, and $[N_{4444}]^+$ have lower predicted $\ln\gamma^{\infty}$ for PFOA and PFOS than the others. In addition, ILs with anions like $[Gly]^-$, $[OAc]^-$, $[2\text{-}OP]^-$, $[CPC]^-$, and $[CHC]^-$ also have a lower $\ln\gamma^{\infty}$ for PFOA and PFOS. Consequently, ILs like $[P_{8884}][Gly]$, $[EMPyrr][Gly]$ and $[EMPyrr][OAc]$ show an exceptionally low $\ln\gamma^{\infty}$ value. The names and structures of cations and anions of ILs used here are shown in Appendix A Tables S2 and S3. The σ surfaces for these cations and anions show the COSMO-RS charge density distribution of the molecule, where the red and blue parts of the molecule represent the negative and positive molecular charge density, respectively. Anions such as $[Gly]^-$ and $[OAc]^-$ contain strongly negative charge densities, which provide sufficiently high σ for hydrogen bonding. As should be noted, once the screening charge density exceeds 0.0082 e/Å^2, it is considered to be polar (Rezaei Motlagh et al., 2019). Common cations that exhibit good solubility for PFOA and PFOS are non-polar molecules such as $[N_{1111}]^+$ and $[N_{4444}]^+$, because they can interact with PFOA and PFOS *via* VdW forces, as shown in our previous work (Zhang et al., 2021).

In contrast to the $\ln\gamma^{\infty}$ for PFOA and PFOS in ILs, the desired $\ln\gamma^{\infty}$ of water in ILs should be high, as severe emulsification may form if water is partially dissolved in ILs. According to the report of Khan et al. (2014), the solubility property of water in ILs can be divided into three regions: (1) $\ln\gamma^{\infty} < -2.2$, water is completely soluble in ILs; (2) $-2.2 \leq \ln\gamma^{\infty} \leq -0.03$, water is partially dissolved in ILs; and (3) $\ln\gamma^{\infty} > -0.03$, water is insoluble in ILs. Thus, for the screening of ILs, $\ln\gamma^{\infty}$ of water more than -0.03 is strongly recommended. In combination with the soluble region of PFOA and PFOS in ILs, 43 ILs were identified as potential candidates for extracting PFOA and PFOS from water. They include the following cations $[N_{8881}(NH_2)_2]^+$, $[N_{8888}]^+$, $[N_{8881}]^+$, $[N_{4444}]^+$, $[N_{11116}]^+$, $[P_{66614}]^+$, $[P_{8884}]^+$, $[P_{4442}]^+$, $[P_{2228}]^+$, $[P_{4442}OH]^+$, $[C_8Mmim]^+$, and these anions $[BH_2(CN)_2]^-$, $[BF_4]^-$, $[B(CN)_4]^-$, $[Tf_2N]^-$, $[ClO_4]^-$, $[I]^-$ (Table 1). The names and structures of cations and anions of ILs used here are shown in Appendix A Tables S2 and S3. Of these, the ILs containing $[I]^-$ anion were reported to undergo hydrolysis in water, which prevents them from being considered further in this work.

2.2. *Experimental validation*

As seen in Table 1, the activity coefficients exhibit a wide range of variation. Therefore, we selected ILs with a range of distribution coefficients to check the applicability of COSMO-RS. Based on the predicted results, these cations $[N_{8881}]^+$, $[N_{1114}]^+$, $[BMIM]^+$, and these anions of $[Tf_2N]^-$, $[BF_4]^-$, $[PF_6]^-$ were selected. For the selected 8 ILs, $[N_{8881}][Tf_2N]$ and $[N_{8881}][BF_4]$ come from the optimized region of $\ln\gamma^{\infty}$ of water more than -0.03, while for the rest of 6 ILs of $[N_{8881}][PF_6]$, $[N_{1114}][Tf_2N]$, $[N_{1114}][BF_4]$, $[N_{1114}][PF_6]$, $[BMIM][BF_4]$, $[BMIM][PF_6]$ of $-2.2 \leq \ln\gamma^{\infty} \leq -0.03$ to verify the prediction results. The experimental values of D_{exp} of PFOA or PFOS of these 8 ILs and pure octanol extractants are listed in Table 2.

From Table 2, the D_{exp} for ILs was up to 5 times higher than the D_{exp} pure octanol, indicating that ILs were superior extractants. In Fig. 3, the COSMO-RS model predictions $\ln D^*_{pre}$ are compared with the experimental data $\ln D_{exp}$, it can be seen that the correlation coefficients were 0.90 and 0.95 between $\ln D_{exp}$ and $\ln D^*_{pre}$ for PFOA and PFOS, respectively, indicating that $\ln D_{exp}$ and $\ln D^*_{pre}$ are linearly correlated, which is in agreement with the theoretical Eq. (3). Meanwhile, the $\ln D^*_{pre}$ values of PFOS were always higher than those of PFOA, meaning PFOS is easier to be extracted than that of PFOA, which is also consistent with the results for $\ln D_{exp}$. The detailed data

Table 1 – Logarithmic infinite dilution activity coefficient ($\ln\gamma^{\infty}$) of PFOA and PFOS in selected ILs (Appendix A Tables S2 and S3) at 298 K.

No.	ILs	$\ln\gamma^{\infty}$		
		PFOA	PFOS	H_2O
1	$[N_{8881}(NH_2)_2][BH_2(CN)_2]$	−8.42	−8.95	−1.20
2	$[P_{66614}][BH_2(CN)_2]$	−4.13	−4.31	1.03
3	$[P_{8884}][BH_2(CN)_2]$	−4.03	−4.16	0.88
4	$[N_{8888}][BH_2(CN)_2]$	−3.96	−4.10	0.92
5	$[N_{8881}][BH_2(CN)_2]$	−3.49	−3.56	0.79
6	$[N_{8881}][I]$	−3.39	−3.19	0.12
7	$[N_{4444}][BH_2(CN)_2]$	−3.26	−3.20	0.46
8	$[P_{4442}][BH_2(CN)_2]$	−2.68	−2.53	0.39
9	$[P_{2228}][BH_2(CN)_2]$	−2.40	−2.24	0.40
10	$[N_{11116}][BH_2(CN)_2]$	−2.02	−1.92	0.62
11	$[P_{66614}][BF_4]$	−1.84	−1.86	1.75
12	$[P_{66614}][B(CN)_4]$	−1.77	−1.87	2.40
13	$[P_{8884}][BF_4]$	−1.76	−1.75	1.57
14	$[P_{8884}][B(CN)_4]$	−1.74	−1.82	2.25
15	$[N_{8888}][BF_4]$	−1.73	−1.72	1.59
16	$[P_{4442}OH][BH_2(CN)_2]$	−1.70	−1.50	0.20
17	$[N_{8888}][B(CN)_4]$	−1.70	−1.78	2.24
18	$[C_8Mmim][BH_2(CN)_2]$	−1.52	−1.28	0.41
19	$[N_{8881}][B(CN)_4]$	−1.39	−1.41	0.79
20	$[N_{4444}][Tf_2N]$	−1.34	−1.43	2.40
21	$[N_{8881}][BF_4]$	−1.31	−1.22	1.39
22	$[P_{8884}][Tf_2N]$	−1.29	−1.43	2.80
23	$[N_{8881}(NH_2)][B(CN)_4]$	−1.29	−1.32	1.94
24	$[N_{4444}][B(CN)_4]$	−1.24	−1.18	1.84
25	$[N_{8888}][Tf_2N]$	−1.21	−1.35	2.77
26	$[P_{66614}][Tf_2N]$	−1.19	−1.33	2.93
27	$[N_{8881}(NH_2)][BF_4]$	−1.18	−1.08	1.28
28	$[N_{4444}][BF_4]$	−1.15	−0.96	1.06
29	$[N_{8881}][Tf_2N]$	−1.12	−1.23	2.61
30	$[P_{4442}][Tf_2N]$	−1.12	−1.18	2.29
31	$[N_{8881}(NH_2)][Tf_2N]$	−1.03	−1.13	2.43
32	$[P_{2228}][Tf_2N]$	−0.97	−1.02	2.23
33	$[P_{4442}][B(CN)_4]$	−0.76	−0.63	1.73
34	$[P_{4442}OH][Tf_2N]$	−0.69	−0.68	0.99
35	$[P_{4442}][BF_4]$	−0.67	−0.39	0.92
36	$[C_8Mmim][Tf_2N]$	−0.57	−0.59	2.15
37	$[P_{2228}][B(CN)_4]$	−0.54	−0.40	1.70
38	$[N_{11116}][Tf_2N]$	−0.54	−0.56	2.23
39	$[P_{66614}][ClO_4]$	−0.52	−0.40	2.38
40	$[P_{2228}][BF_4]$	−0.41	−0.11	0.90
41	$[N_{8888}][ClO_4]$	−0.40	−0.25	2.21
42	$[P_{8884}][ClO_4]$	−0.40	−0.24	2.21
43	$[N_{11116}][B(CN)_4]$	−0.31	−0.19	1.77

of $\ln D^*_{pre}$ for PFOA and PFOS are listed in Appendix A Tables S5 and S6, respectively, and the corresponding 3D plots are illustrated in Appendix A Fig. S1. For ILs with the same cation but different anions, the relative difference in $\ln D^*_{pre}$ values was significantly larger than ILs with the same anion but different cations, indicating that the predicted $\ln D^*_{pre}$ was more sensitive to the types of anions rather than to the cations. For example, for ILs with the same cation $[N_{8881}]^+$, the $\ln D^*_{pre}$ values for PFOA were +26.42 for $[N_{8881}][Gly]$ and +12.52 for $[N_{8881}][Tf_2N]$ (Appendix A Table S5). And for PFOS they were +29.13 for $[N_{8881}][Gly]$ and +14.86 for $[N_{8881}][Tf_2N]$ (Appendix A Table S6). For ILs with the same anion, the $\ln D^*_{pre}$ values for

Table 2 – Experimental results (extraction percentage *E*, distribution coefficient D_{exp}) for PFOA and PFOS.

No.	ILs	PFOA		PFOS	
		E (%)	D_{exp}	*E* (%)	D_{exp}
1	$[N_{8881}][Tf_2N]$	33.70	0.51	49.50	0.98
2	$[N_{8881}][BF_4]$	25.60	0.34	38.20	0.62
3	$[N_{8881}][PF_6]$	16.60	0.20	28.10	0.39
4	$[N_{1114}][Tf_2N]$	8.60	0.09	22.30	0.29
5	$[N_{1114}][BF_4]$	5.10	0.05	12.50	0.14
6	$[N_{1114}][PF_6]$	1.80	0.02	6.20	0.07
7	$[BMIM][BF_4]$	12.50	0.14	19.30	0.24
8	$[BMIM][PF_6]$	7.80	0.08	15.60	0.18
9	Pure octanol	1.96	0.02	3.85	0.04

ILs refer to Appendix A Tables S2 and S3. Experimental conditions: concentration of IL 1.25 mmol/L (about 10 times of the solute), concentration of PFOA or PFOS 50 mg/L, volume ratio of the organic solution to the aqueous solution 1:1, temperature 298 K, and extraction time 30 min.

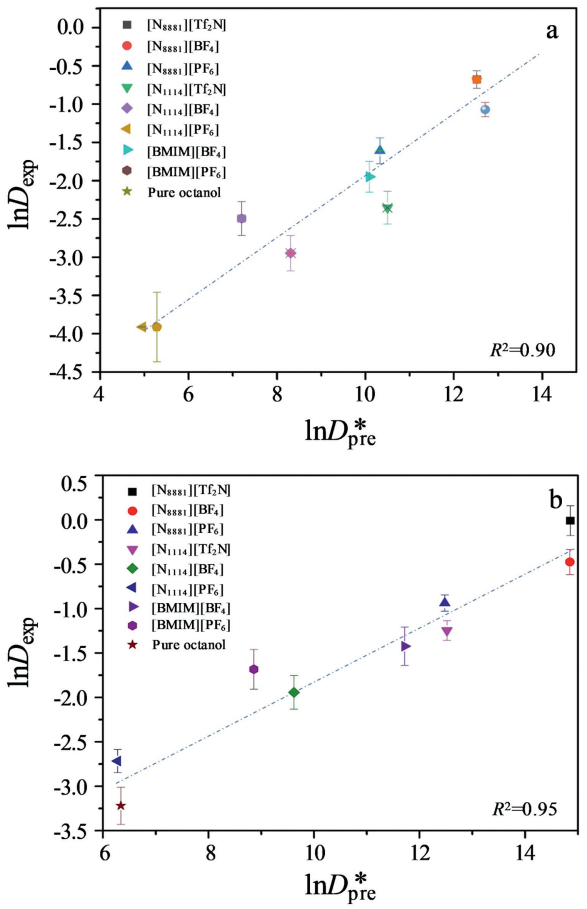

Fig. 3 – Logarithmic of the proportional relative value of the actual distribution coefficient ($\ln D^*_{pre}$) and the logarithmic of experimental distribution coefficient ($\ln D_{exp}$) of 8 selected ILs for (a) PFOA and (b) PFOS extraction.

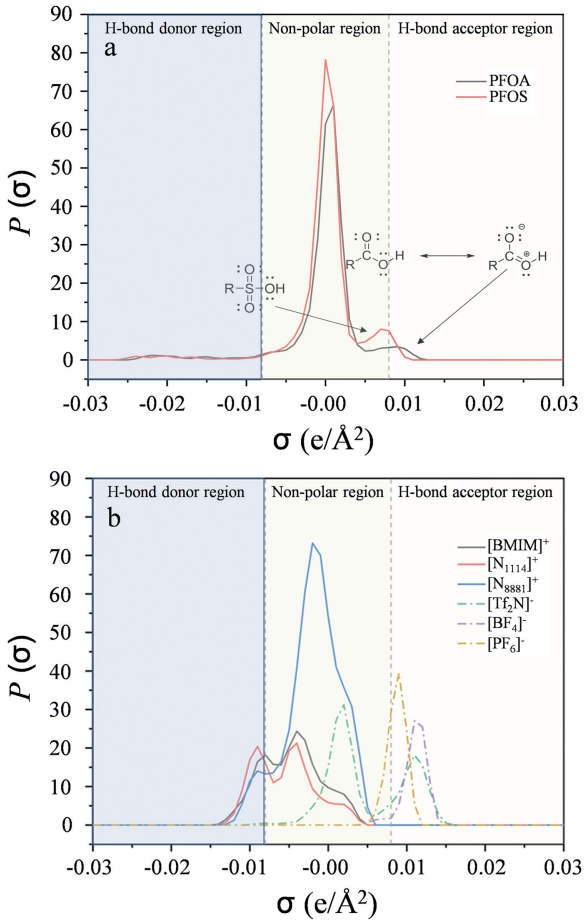

Fig. 4 – σ-profiles of (a) PFOA, PFOS, and (b) cations and anions of different ILs. *P*(σ): the probability distribution of a specific charge density.

PFOA varied from +26.42 of $[N_{8881}][Gly]$ to +26.58 of $[P_{4442}][Gly]$ (Appendix A Table S5), while $\ln D^*_{pre}$ values of PFOS were +29.13 for $[N_{8881}][Gly]$ and +29.64 for $[P_{4442}][Gly]$ (Appendix A Table S6). Therefore, it can be concluded from the predicted $\ln D^*_{pre}$ values that anion selection significantly influences the extraction of PFOA and PFOS from water using ILs.

In general, as both PFOA and PFOS are present in water, thus the selectivity of the ILs is of great important. The higher the selectivity (S_{pre}), the easier it is to extract PFOA or PFOS from the wastewater. Appendix A Fig. S2 shows the predicted logarithmic selectivity ($\ln S^*_{pre}$) of PFOA to PFOS in ILs at 298.15 K. It is obvious that $\ln S^*_{pre}$ of PFOA with respect to PFOS is always less than zero. The results indicate that the selectivity of PFOS in ILs is higher than that of PFOA, which is generally consistent with the experimental results. Take $[N_{8881}][Tf_2N]$, $[N_{8881}][BF_4]$, [BMIM][BF_4], and [BMIM][PF_6] as examples, the $\ln S^*_{pre}$ values of $[N_{8881}][Tf_2N]$ and $[N_{8881}][BF_4]$ are 2.35 and 2.15, respectively, showing the same tendency with the experimental $\ln D_{exp}$.

To gain a deeper understanding of D^*_{pre} and D_{exp}, we then analyzed the σ-profiles, as shown in Fig. 4a. In the H-bond donor region, PFOA and PFOS generally had very similar σ-profiles, whereas when it came to the non-polar region, it is evident that PFOS was larger than that of PFOA. For the polar region, the positive electron distribution of PFOA exceeded 0.0082 e/Å^2 due to the presence of two equivalent resonance structures in which the negative charge was delocalized over two O atoms. By contrast, for PFOS, the sulfonic acid group lacked stable resonance structures, which made PFOA a stronger H-bond acceptor than PFOS. The σ-profiles can be broken down into misfit (MF) interaction energy, H-bond (HB) interaction energy, and VdW interaction energy, and the results are shown in Appendix A Table S7. The dominant interactions for PFOA and PFOS are VdW forces, which are related to the non-polar region. PFOS had a higher VdW interaction energy compared to PFOA, which explained well why D_{exp} and D^*_{pre} were higher for PFOS than PFOA.

The σ-profiles of the cations and anions of ILs were also analyzed. As previously discussed, PFOA and PFOS are strong H-bond acceptors. Accordingly, PFOA and PFOS are stabilized by a positive electron donor, which is shown on the right side of the σ-profiles. As shown in Fig. 4b, the peaks of $[Tf_2N]^-$ and $[BF_4]^-$ are more positive than those of $[PF_6]^-$. Thus, the extraction efficiency of $[PF_6]^-$ is lower than that of the other two ILs. Notably, as the VdW forces are dominant, cations with σ-profile area in the non-polar region are beneficial for extraction. As a result, the ILs containing $[N_{8881}]^+$ cations showed the highest extraction efficiency among the other three cationic ILs.

3. Conclusions

In this work, the COSMO-RS method was employed to screen potential ILs to extract PFOA and/or PFOS from aqueous solutions. According to the screening results on the basis of the calculation of the infinite dilution activity coefficient (γ^∞), the ILs with H-bond acceptors in both anions and cations are favorable as extractants. Eight ILs with cations of $[N_{8881}]^+$, $[N_{1444}]^+$, and $[BMIM]^+$, and with the anions of $[Tf_2N]^-$, $[BF_4]^-$ and $[PF_6]^-$ were selected for the extraction of PFOA and PFOS. The extraction performance indicated that the ILs with the cation of $[N_{8881}]^+$ given the best extraction result in order of $[N_{8881}][Tf_2N] > [N_{8881}][BF_4] > [N_{8881}][PF_6]$. Further analysis of the σ-profiles demonstrated that VdW forces play a crucial role in the extraction of PFOS and PFOA, followed by misfit and H-bond interactions. In conclusion, this work provided a fast and reliable method for screening the potential ILs for the extraction of PFACs from wastewater, offering a promising alternative way for the treatment of persistent organic pollutants (POPs) using ILs.

Declaration of Competing Interest

The authors declare that they have no known competing financial interests or personal relationships that could have appeared to influence the work reported in this article.

Acknowledgments

The authors appreciate the support from the Brook Byers Institute for Sustainable Systems, Hightower Chair, and Georgia

Research Alliance at the Georgia Institute of Technology. The views and ideas expressed herein are solely those of the authors and do not represent the ideas of the funding agencies in any form.

Appendix A Supplementary data

Supplementary material associated with this article can be found in the online version at doi:10.1016/j.jes.2022.08.025.

REFERENCES

Arenas, P., Suarez, I., Coto, B., 2022. Combination of molecular dynamics simulation, COSMO-RS, and experimental study to understand extraction of naphthenic acid. Sep. Purif. Technol. 280, 119810.

Arias, E.V., Mallavarapu, M., Naidu, R., 2015. Identification of the source of PFOS and PFOA contamination at a military air base site. Environ. Monit. Assess. 187, 4111.

Austin, N.D., Sahinidis, N.V., Konstantinov, I.A., Trahan, D.W., 2018. COSMO-based computer-aided molecular/mixture design: a focus on reaction solvents. AIChE J. 64, 104–122.

Badruddoza, A.Z.M., Bhattarai, B., Suri, R.P.S., 2017. Environmentally friendly β-cyclodextrin–ionic liquid polyurethane-modified magnetic sorbent for the removal of PFOA, PFOS, and Cr(VI) from water. ACS Sust. Chem. Eng. 5, 9223–9232.

Bao, Y., Deng, S., Jiang, X., Qu, Y., He, Y., Liu, L., et al., 2018. Degradation of PFOA substitute: GenX (HFPO–DA ammonium salt): oxidation with UV/persulfate or reduction with UV/sulfite? Environ. Sci. Technol. 52, 11728–11734.

Bao, Y., Niu, J., Xu, Z., Gao, D., Shi, J., Sun, X., et al., 2014. Removal of perfluorooctane sulfonate (PFOS) and perfluorooctanoate (PFOA) from water by coagulation: mechanisms and influencing factors. J. Colloid. Interface Sci. 434, 59–64.

Bentel, M.J., Liu, Z., Yu, Y., Gao, J., Men, Y., Liu, J., 2020. Enhanced degradation of perfluorocarboxylic acids (PFCAs) by UV/sulfite treatment: Reaction mechanisms and system efficiencies at pH 12. Environ. Sci. Technol. Lett. 7, 351–357.

Brouwer, T., Schuur, B., 2019. Model performances evaluated for infinite dilution activity coefficients prediction at 298.15 K. Ind. Eng. Chem. Res. 58, 8903–8914.

Chen, W., Zhang, X., Mamadiev, M., Wang, Z., 2017. Sorption of perfluorooctane sulfonate and perfluorooctanoate on polyacrylonitrile fiber-derived activated carbon fibers: In comparison with activated carbon. RSC Adv. 7, 927–938.

Chen, Z., Zhang, H., Li, H., Xu, Y., Shen, Y., Zhu, Z., et al., 2021. Separation of n-heptane and tert-butanol by ionic liquids based on COSMO-SAC model. Green Energy Environ. 6, 380–391.

Chiavola, A., Di Marcantonio, C., Boni, M.R., Biagioli, S., Frugis, A., Cecchini, G., 2020. Experimental investigation on the perfluorooctanoic and perfluorooctane sulfonic acids fate and behaviour in the activated sludge reactor. Process. Saf. Environ. 134, 406–415.

Costanza, J., Arshadi, M., Abriola, L.M., Pennell, K.D., 2019. Accumulation of PFOA and PFOS at the air–water interface. Environ. Sci. Technol. Lett. 6, 487–491.

Coto, B., Suárez, I., Tenorio, M.J., Nieto, S., Alvarez, N., Peña, J.L., 2021. Oil acidity reduction by extraction with imidazolium ionic liquids: Experimental, COSMO description and reutilization study. Sep. Purif. Technol. 254, 117529.

Dai, C., Qi, Z., Lei, Z., Palomar, J., 2021. COSMO-based models. Green Energy Environ. 6, 309–310.

Droge, S.T.J., 2019. Membrane–water partition coefficients to aid risk assessment of perfluoroalkyl anions and alkyl sulfates. Environ. Sci. Technol. 53, 760–770.

Eckert, F., Klamt, A., 2002. Fast solvent screening via quantum chemistry: COSMO-RS approach. AIChE J. 48, 369–385.

Goss, K.-U., 2008. The pKa values of PFOA and other highly fluorinated carboxylic acids. Environ. Sci. Technol. 42, 456–458.

Jiang, C., Cheng, H., Qin, Z., Wang, R., Chen, L., Yang, C., et al., 2021. COSMO-RS prediction and experimental verification of 1,5-pentanediamine extraction from aqueous solution by ionic liquids. Green Energy Environ. 6, 422–431.

Khan, I., Kurnia, K.A., Mutelet, F., Pinho, S.P., Coutinho, J.A.P., 2014. Probing the interactions between ionic liquids and water: Experimental and quantum chemical approach. J. Phys. Chem. B 118, 1848–1860.

Klamt, A., Eckert, F., Arlt, W., 2010. COSMO-RS: an alternative to simulation for calculating thermodynamic properties of liquid mixtures. Annu. Rev. Chem. Biomol. Eng. 1, 101–122.

Kurnia, K.A., Quental, M.V., Santos, L.M.N.B.F., Freire, M.G., Coutinho, J.A.P., 2015. Mutual solubilities between water and non-aromatic sulfonium-, ammonium- and phosphonium-hydrophobic ionic liquids. Phys. Chem. Chem. Phys. 17, 4569–4577.

Li, B., Wang, C., Zhang, Y., Wang, Y., 2021. High CO_2 absorption capacity of metal-based ionic liquids: A molecular dynamics study. Green Energy Environ. 6, 253–260.

Li, Z., Li, R., Yuan, X., Pei, Y., Zhao, Y., Wang, H., et al., 2019. Anionic structural effect in liquid–liquid separation of phenol from model oil by choline carboxylate ionic liquids. Green Energy Environ. 4, 131–138.

Lin, H., Niu, J., Liang, S., Wang, C., Wang, Y., Jin, F., et al., 2018. Development of macroporous Magnéli phase Ti_4O_7 ceramic materials: as an efficient anode for mineralization of poly- and perfluoroalkyl substances. Chem. Eng. J. 354, 1058–1067.

Liu, Y., Dai, Z., Zhang, Z., Zeng, S., Li, F., Zhang, X., et al., 2021. Ionic liquids/deep eutectic solvents for CO_2 capture: reviewing and evaluating. Green Energy Environ. 6, 314–328.

Liu, Y., Yu, H., Sun, Y., Zeng, S., Zhang, X., Nie, Y., et al., 2020. Screening deep eutectic solvents for CO_2 capture with COSMO-RS. Front. Chem. 8, 82.

Louwen, J.N., Pye, C.C., van Lenthe, E., Austin, N.D., McGarrity, E.S., Xiong, R., et al., 2020. AMS 2020 COSMO-RS, SCM, Theoretical Chemistry. Vrije Universiteit, Amsterdam, The Netherlands.

Mullins, E., Oldland, R., Liu, Y.A., Wang, S., Sandler, S.I., Chen, C.-C., et al., 2006. Sigma-profile database for using COSMO-based thermodynamic methods. Ind. Eng. Chem. Res. 45, 4389–4415.

Niu, J., Li, Y., Shang, E., Xu, Z., Liu, J., 2016. Electrochemical oxidation of perfluorinated compounds in water. Chemosphere 146, 526–538.

Olea, F., Merlet, G., Araya-López, C., Cabezas, R., Villarroel, E., Quijada-Maldonado, E., et al., 2021. Separation of vanillin by perstraction using hydrophobic ionic liquids as extractant phase: analysis of mass transfer and screening of ILs via COSMO-RS. Sep. Purif. Technol. 274, 119008.

Pye, C.C., Ziegler, T., van Lenthe, E., Louwen, J.N., 2009. An implementation of the conductor-like screening model of solvation within the Amsterdam density functional package - Part II. COSMO for real solvents (1). Can. J. Chem. 87, 790–797.

Qian, Y., Guo, X., Zhang, Y., Peng, Y., Sun, P., Huang, C.-H., et al., 2016. Perfluorooctanoic acid degradation using UV-persulfate process: modeling of the degradation and chlorate formation. Environ. Sci. Technol. 50, 772–781.

Rezaei Motlagh, S., Harun, R., Awang Biak, D.R., Hussain, S.A., Wan Ab Karim Ghani, W.A., Khezri, R., et al., 2019. Screening of suitable ionic liquids as green solvents for extraction of eicosapentaenoic acid (EPA) from microalgae biomass using COSMO-RS model. Molecules 24, 713.

Rezaei Motlagh, S., Harun, R., Radiah Awang Biak, D., Hussain, S.A., Elgharbawy, A.A., Khezri, R., et al., 2020. Prediction of potential ionic liquids (ILs) for the solid-liquid extraction of docosahexaenoic acid (DHA) from microalgae using COSMO-RS screening model. Biomolecules 10, 1149.

Schwarzenbach, R.P., Gschwend, P.M., Imboden, D.M., 2016. Environmental Organic Chemistry. John Wiley & Sons.

Senevirathna, S.T.M.L.D., Tanaka, S., Fujii, S., Kunacheva, C., Harada, H., Ariyadasa, B.H.A.K.T., et al., 2010. Adsorption of perfluorooctane sulfonate (n-PFOS) onto non ion-exchange polymers and granular activated carbon: Batch and column test. Desalination 260, 29–33.

Skoronski, E., Fernandes, M., Malaret, F.J., Hallett, J.P., 2020. Use of phosphonium ionic liquids for highly efficient extraction of phenolic compounds from water. Sep. Purif. Technol. 248, 117069.

Song, M., Zhang, W., Chen, Y., Luo, J., Crittenden, J.C., 2017. The preparation and performance of lignin-based activated carbon fiber adsorbents for treating gaseous streams. Front. Chem. Sci. Eng. 11, 328–337.

Sun, W., Wang, M., Zhang, Y., Ding, W., Huo, F., Wei, L., et al., 2020. Protic *vs* aprotic ionic liquid for CO_2 fixation: A simulation study. Green Energy Environ. 5, 183–194.

Wang, T., Wang, Y., Liao, C., Cai, Y., Jiang, G., 2009. Perspectives on the inclusion of perfluorooctane sulfonate into the stockholm convention on persistent organic pollutants. Environ. Sci. Technol. 43, 5171–5175.

Wang, Z., MacLeod, M., Cousins, I.T., Scheringer, M., Hungerbühler, K., 2011. Using COSMOtherm to predict physicochemical properties of poly- and perfluorinated alkyl substances (PFASs). Environ. Chem. 8, 389–398.

Wu, Z., Shi, S., Zhan, G., Chang, F., Bai, Y., Zhang, X., et al., 2021. Ionic liquid screening for dichloromethane absorption by multi-scale simulations. Sep. Purif. Technol. 275, 119187.

Xiong, R.C., Sandler, S.I., Burnett, R.I., 2014. An improvement to COSMO-SAC for predicting thermodynamic properties. Ind. Eng. Chem. Res. 53, 8265–8278.

Yokozeki, A., Shiflett, M.B., 2010. Water solubility in ionic liquids and application to absorption cycles. Ind. Eng. Chem. Res. 49, 9496–9503.

Zhang, K., Kujawski, D., Spurrell, C., Wang, D., Yan, J., Crittenden, J.C., 2021. Extraction of PFOA from dilute wastewater using ionic liquids that are dissolved in N-octanol. J. Hazard. Mater. 404, 124091.

Zhang, S., 2020. COIL-8: Ionic liquids for tomorrow. Green Energy Environ. 5, 121.

Zhao, D., Liu, C., Wang, Y., Zhang, H., 2022. Ionic liquids design for efficient separation of anthracene and carbazole. Sep. Purif. Technol. 281, 119892.

Zhou, Z., Liang, Y., Shi, Y., Xu, L., Cai, Y., 2013. Occurrence and transport of perfluoroalkyl acids (PFAAs), including short-chain PFAAs in Tangxun Lake, China. Environ. Sci. Technol. 47, 9249–9257.